Available online at www.sciencedirect.com

ScienceDirect

Solar Energy 84 (2010) 79–89

SOLAR ENERGY

www.elsevier.com/locate/solener

A reliable, fast and low cost maximum power point tracker for photovoltaic applications

J.M. Enrique *, J.M. Andújar, M.A. Bohórquez

Departamento de Ingeniería Electrónica, de Sistemas Informáticos y Automática, Universidad de Huelva, Spain

Received 19 February 2009; received in revised form 22 July 2009; accepted 16 October 2009
Available online 14 November 2009

Communicated by: Associate Editor Elias Stefanakos

Abstract

This work presents a new maximum power point tracker system for photovoltaic applications. The developed system is an analog version of the "P&O-oriented" algorithm. It maintains its main advantages: simplicity, reliability and easy practical implementation, and avoids its main disadvantages: inaccurateness and relatively slow response. Additionally, the developed system can be implemented in a practical way at a low cost, which means an added value. The system also shows an excellent behavior for very fast variables in incident radiation levels.

Keywords: Analog system; Efficiency; Low cost; Maximum power point tracker; Photovoltaic array; "P&O" algorithm

1. Introduction

In the specialized literature numerous proposals of MPP tracking systems can be found. Most of them have similar efficiency, which can also be considered acceptable for most applications. As a result, the interest of the authors when implementing this work has focused on achieving a certain added value in the proposed system, which can be found in the accurateness, speed and low cost. This allows its application even to household installations, where investment costs may be the most determining factor for decision making. The developed system presents the advantage of its high speed which also helps to improve the photovoltaic system efficiency.

A photovoltaic (PV) array that functions under uniform radiation and temperature conditions presents an I–V and P–V characteristic as the one shown in Figs. 1(a) and (b), respectively. As can be observed, there is a single point, called "MPP" (Maximum Power Point), where the array provides the maximum power possible for these environmental conditions (radiation and temperature), and so functions with the maximum performance. When a load is connected directly to a PV array (direct coupling), the operation point is defined by the intersection of its I–V characteristics, as shown in Fig. 1(a).

In general, this operation point does not coincide with the MPP. Thus, in direct coupling systems, the array must be over-dimensioned to guarantee the power demand of the load. Obviously, this implies a more expensive system. To solve this problem, a DC/DC (Xiao et al., 2007) converter with an algorithm for the automatic control of its duty cycle "δ" is inserted between the photovoltaic array and the load (see Fig. 2), resulting in what is known as MPPT (Maximum Power Point Tracker) system.

The MPPT must control the voltage or current (through the δ of the converter) of the PV array regardless of the

* Corresponding author. Address: Departamento de Ingeniería Electrónica, de Sistemas Informáticos y Automática, Universidad de Huelva, Huelva, Spain. Tel.: +34 959 217374/7656/7671; fax: +34 959 217348.

E-mail addresses: juanm.enrique@diesia.uhu.es (J.M. Enrique), andujar@diesia.uhu.es (J.M. Andújar), bohorquez@diesia.uhu.es (M.A. Bohórquez).

0038-092X/$ - see front matter
doi:10.1016/j.solener.2009.10.011

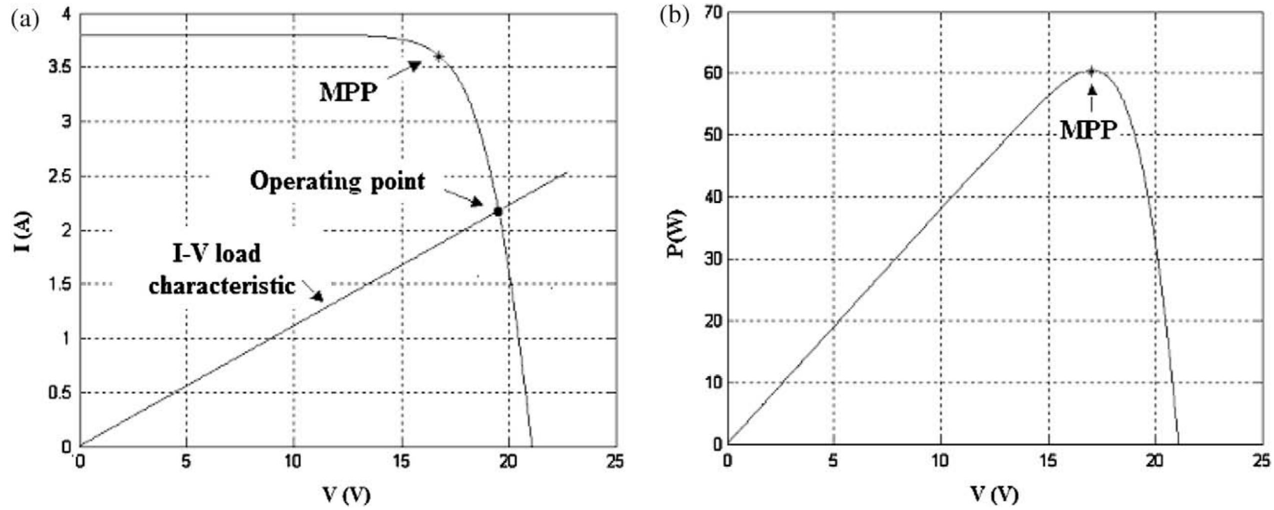

Fig. 1. (a) I–V characteristic of a PV array, MPP and system operation point. (b) P–V characteristic of the PV array.

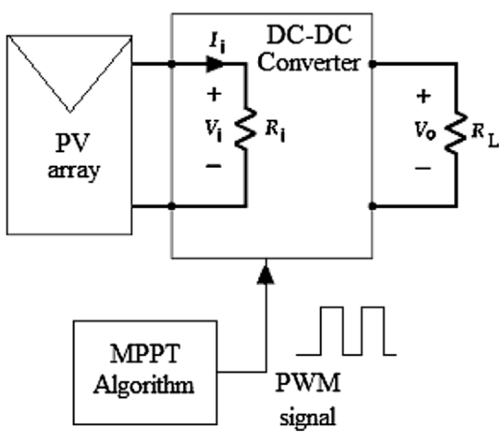

Fig. 2. Basic diagram of an MPPT system.

load, trying to place it in the MPP. The DC/DC converter presents an input impedance (R_i) which depends basically on the load impedance (R_L) and the duty cycle (δ) (Enrique et al., 2005a,b, 2007; Durán et al., 2008, 2009). Therefore, the MPPT must find the optimal δ for the operation point of the PV array to coincide with the maximum power point (MPP).

Although the solution to operating in the MPP may seem immediate, it is not. This is because the location of the MPP in the I–V curve of the PV array is not known *a priori*. This point must be located, either by mathematical calculations over a valid model, or by using some search algorithm. This implies even more difficulty if we consider the fact that the MPP presents non-linear dependencies with temperature and radiation, as observed in Fig. 3.

Fig. 3(a) shows a set of I–V curves for different levels of radiation and constant temperature. In Fig. 3(b), the same set of curves is presented at a higher temperature. Observe the change in the voltage and, especially, in the current of the MPP.

Numerous MPPT algorithms have been proposed and developed in the literature. Among them, the "Perturbation and Observation (P&O)" algorithm is probably the most

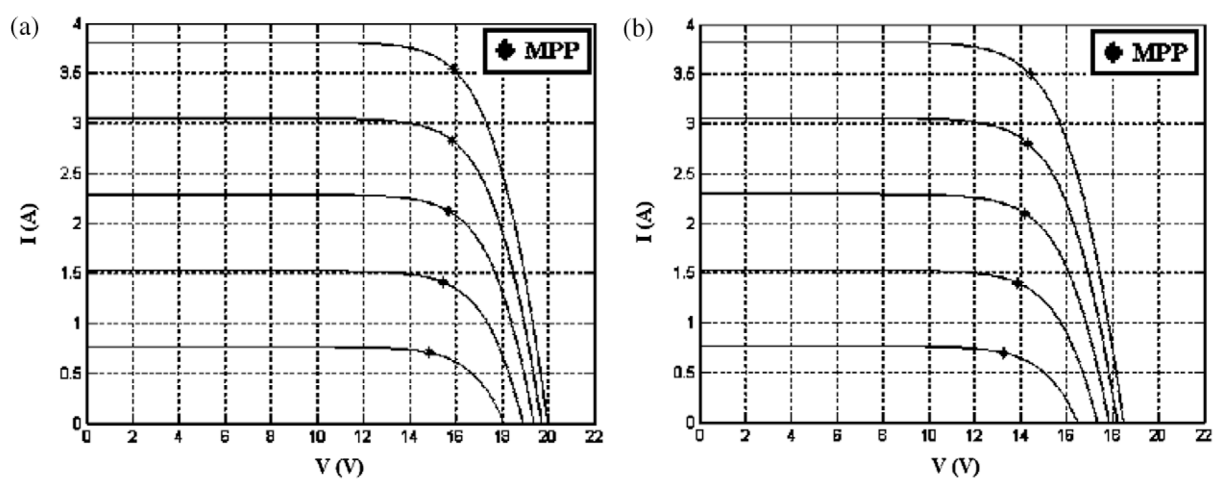

Fig. 3. (a) I–V characteristic of a PV array at 40 °C and different radiation levels (200–400 to 600–800 and 1000 W/m^2). (b) I–V characteristic of a PV array at 60 °C and different radiation levels (200–400 to 600–800 and 1000 W/m^2).

extensively used in commercial MPPT systems. However, there is no clear agreement on which algorithm is best. Hohm and Ropp (2002) presented a study that basically concludes with not very different performances for most of the different algorithms and where the traditional P&O is quite successful.

To establish the quality of a given MPPT system (and to be able to compare it with other systems), it is necessary to define the "*tracking efficiency* (η)", given by Eq. (1) (Hohm and Ropp, 2002):

$$\eta_{MPPT} = \frac{\int_0^t P_{inst}(t)dt}{\int_0^t P_{max}(t)dt} \tag{1}$$

where, for radiation and temperature conditions in the given time period, $P_{inst}(t)$ is the instantaneous power supplied by the MPPT system controlled PV array, and $P_{max}(t)$ is the actual MPP power.

2. Algorithms for MPP tracking

A very short revision of the most usual algorithms for MPP tracking is presented below.

2.1. Perturbation and Observation (P&O)

The Perturbation and Observation (P&O) algorithm is probably the most frequently used in practice, mainly due to its easy implementation (Kim et al., 1996). Its operation is briefly explained as follows: assume that the PV array operates at a given point, which is outside the MPP. The PV array operational voltage is perturbed by a small ΔV, and then the change in the power (ΔP) is measured. If $\Delta P > 0$, the operation point has approached the MPP, and therefore, the next perturbation must take place in the same direction as the previous one (same algebraic sign). If, on the contrary, $\Delta P < 0$, the system has moved away from the MPP and, consequently, the next perturbation must be performed in the opposite direction (opposed algebraic sign).

As stated before, the advantages of this algorithm are its simplicity and easy implementation. However, it has limitations that reduce its tracking efficiency. When the light intensity decreases considerably, the P–V curve becomes very flat. This makes it difficult for the MPPT to locate the MPP, since the changes that take place in the power are small as regards perturbations occurred in the voltage.

Another disadvantage of the "P&O" algorithm is that it cannot determine when it has exactly reached the MPP. Thus, it remains oscillating around it, changing the sign of the perturbation for each ΔP measured. It has also been observed that this algorithm can show misbehavior under fast changes in the radiation levels (Kawamura et al., 1997).

Several improvements in the "P&O" algorithm have been proposed (Enslin et al., 1997; Andujar et al., 2005; Xiao et al., 2007). One of them is the addition of a waiting time if the system identifies a series of alternate signs in the perturbation, meaning that it is very close to the MPP. This allows reducing the oscillation around the MPP and improves the algorithm efficiency under constant radiation conditions. However, this algorithm causes the MPPT to be very slow, making its misbehavior more noticeable in partly cloudy days.

Other modifications to the "P&O" algorithm, as the ones detailed below, directly affect the perturbation sign according to whether certain conditions are given.

2.1.1. "P&O" oriented algorithm

The "P&O" oriented algorithm (Andujar et al., 2005) is able to distinguish with certain accuracy whether the system is operating to the right or left of the MPP and act consequently, so increasing tracking efficiency. However, it is observed that whenever there is a sudden variation in the incident radiation (caused, for example, by the passing of a cloud) and, therefore, in the power supplied by the photovoltaic generator, the system is unable to distinguish instantaneously the appropriate direction of the change in δ (Hohm and Ropp, 2002). This algorithm is discussed in detailed in Section 3.

2.1.2. "P&O" modified algorithm

To correct the defect caused by sudden radiation variations in the previous algorithm, a slight variation has been proposed (Andujar et al., 2005). As already known, variations in the light radiation have an effect mainly and directly on the current supplied by the photovoltaic array (Alonso, 1998). Thus, an increase in radiation will cause a rise in the value of the MPP current (see Fig. 3). When the algorithm detects a variation in radiation over a certain threshold, its response is an immediate increase in δ. In this way, the DC/DC converter decreases its input impedance R_i, and so obliges the photovoltaic generator to move to higher current points close to the MPP. An advantage of this algorithm is that it does not require precise measurements of radiation (this would remarkably increase the price of its practical implementation), since it only needs the sign of the radiation increase within an interval of measures. A simple photodiode can be useful for this purpose.

2.2. Constant voltage and current

The "Constant Voltage (CV)" algorithm (Hohm and Ropp, 2002; Koizumi et al., 2006) is based on the fact that in the I–V curves of a PV array the ratio between the maximum power point voltage and that of the open circuit is roughly constant (something similar occurs with the ratio between the current of the maximum power point and that of the short circuit) (Noguchi et al., 2002; Mutoh et al., 2006; Mutoh and Inoue, 2007), that is:

$$\frac{V_{MPP}}{V_{OC}} \cong K < 1 \tag{2}$$

where V_{MPP} is the maximum power point voltage and V_{OC} is the open circuit voltage. The PV array is temporarily isolated by the MPPT system to measure V_{OC}. Next, the MPPT calculates the correct operation point using Eq. (2) and adjusts the voltage of the PV array until it reaches the MPP. This operation is repeated periodically to track the MPP.

Although this method is simple, choosing the optimal K value, which, on the other hand, is not totally constant, may be difficult. The literature indicates good values for K within the range 0.73–0.80 (Andersen and Alvsten, 1995; van der Merwe and van der Merwe, 1998; Abou El Ela and Roger, 1984).

This method can be implemented in a relatively easy way using analog software. However, its efficiency is lower than that of other methods (Hohm and Ropp, 2002). The main reasons are:

(I) Errors in the K value.
(II) The measure of V_{OC} (I_{SC}) requires the momentary interruption of the power supplied by the array.

2.3. Incremental conductance

The so called "incremental conductance" method (Hohm and Ropp, 2002) derives directly from the power equation, which will be given in the MPP by:

$$\left.\frac{dP}{dV}\right|_{MPP} = \left.\frac{d(V \cdot I)}{dV}\right|_{MPP} = 0 \Rightarrow -\frac{I}{V} = \frac{dI}{dV} \tag{3}$$

If instantaneous conductance g_L, and increasing conductance g_P, are defined as:

$$g_L = -\frac{I}{V}; \quad g_p = \frac{dI}{dV} \tag{4}$$

Then, expression (3) can be re-written in the form of:

$$\left.\frac{dP}{dV}\right|_{MPP} = 0 \Rightarrow g_L = g_P \tag{5}$$

The previous equation indicates that in the MPP the instantaneous and incremental conductance must be equal. If the operation point does not coincide with the MPP, then a series of inequations directly derived from expression (5) (Hohm and Ropp, 2002; Koizumi et al., 2006) allow us to know whether the operation voltage is higher or lower than V_{MPP}, and so to act consequently.

Once the MPP has been reached, every time a change occurs in the radiation on the array the MPPT will tend to increase or decrease the operation voltage to follow the MPP.

The disadvantage of this method is that it needs a precise calculation of g_L and g_P, which makes the MPPT more difficult and relatively slow.

2.4. Parasitic capacity

This algorithm is similar to the previous one, except that in this algorithm the effect of the parasitic capacity of the junction p–n is included. This effect can be modeled (Brambilla et al., 1998) as a condenser connected between the terminals of each cell. By connecting cells in parallel the parasitic capacity observed by the MPP will increase. As a result, the differences between the tracking efficiencies of the MPP between "Increasing Conductance" and "Parasitic Capacity" algorithms are more outstanding in high power arrays, where there are numerous modules connected in parallel.

The practical implementation of this algorithm is complex, especially for the difficulty entailed by the calculation of increasing conductance g_P. A detailed study of this algorithm is shown in Brambilla et al. (1998).

2.5. Model-based algorithms

If a suitable model is available for a cell or photovoltaic array and there are precise radiation and temperature measures available (which implies a significant increase in the price of the system, although there have recently been developed sensors of temperature and radiation at a low cost (Martínez and Andújar, 2009; Martínez et al., 2009), the MPP voltage and current may be directly calculated by solving equation $dP/dV = 0$ (for example, using a numeric method). Then, the MPPT would just have to adjust voltage and current values to those calculated ones (Xiao et al., 2006).

Even so, the model-based MPPTs are not practical, since the values for the cell parameters are not known with accuracy and, in fact, can vary significantly between cells from the same production series. Moreover, only the cost of a precise light radiation sensor (pyranometer) can cause this MPPT system to be non-viable in practice.

Having revised the most usual algorithms and methods for MPP tracking, it seems that the P&O algorithm and, more specifically, its "oriented" variant, is the one with the best ratio efficiency/easiness of practical implementation. This is mainly due to its proper operation, simplicity and low cost (note that it needs no radiation and temperature sensors). Nonetheless, as already mentioned, it has the disadvantage of its instantaneous confusion when facing sudden variations in the incident radiation. This disadvantage could be overcome with a system fast enough to make its reaction speed higher than the speed of the incident radiation change – which is the main reason in the MPP movement. To achieve this without losing the advantages of the *P&O-oriented* algorithm, the authors have developed a system which is described below.

3. P&O oriented analog system

A completely analog system able to implement the algorithm for MPP tracking, known as "P&O-oriented" algorithm, is presented in this section (Andujar et al., 2005).

3.1. Operation of the P&O-oriented algorithm

Consider Fig. 4, where the P–V characteristic of a photovoltaic array at a given temperature and radiation is

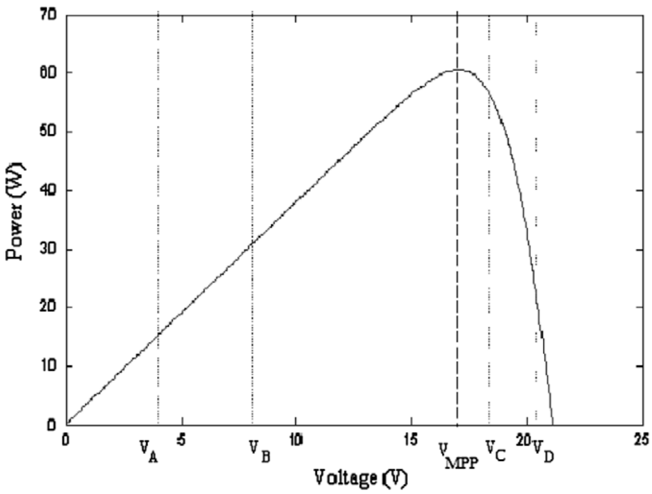

Fig. 4. P–V characteristic of a photovoltaic array. The developed MPPT algorithm is able to distinguish whether the system is operating to the right or left of the MPP and act consequently.

shown. Assume that, due to a modification in the duty cycle (δ) of the converter, the system evolves from V_A to V_B ($\Delta V > 0$ and $\Delta P > 0$). As observed in Fig. 4, the MPP voltage, V_{MPP}, is higher than V_B, and therefore, the output voltage must keep increasing. Now assume that the perturbation has moved the operation point from V_B to V_A. In this case, the voltage of the array must increase again to approach V_{MPP}. All possible combinations are shown in Table 1.

The only variable to which the control system can access is the duty cycle (δ). Any increase in δ implies a decrease in the input resistance R_i of the DC–DC converter (and subsequently, a decrease in the operation voltage of the photovoltaic generator) and vice versa (Enrique et al., 2005a,b, 2007; Durán et al., 2008, 2009). The system starts from an initial value (for example $\delta = 0.5$) that varies at constant increase ($\Delta\delta$) according to expressions (6) and (7).

$$b_i = -sign[(\Delta V) \cdot (\Delta P)] \tag{6}$$

$$\delta_i = \delta_{i-1} + b_i \cdot \Delta\delta \tag{7}$$

In each iteration "i", ΔP and ΔV measures are obtained. Next, the value of δ is adjusted to approach it to the MPP. Note that no temperature and solar radiation measures are needed to do the tracking, which reduces the price of the control system. The flow chart diagram of this algorithm is shown in Fig. 5.

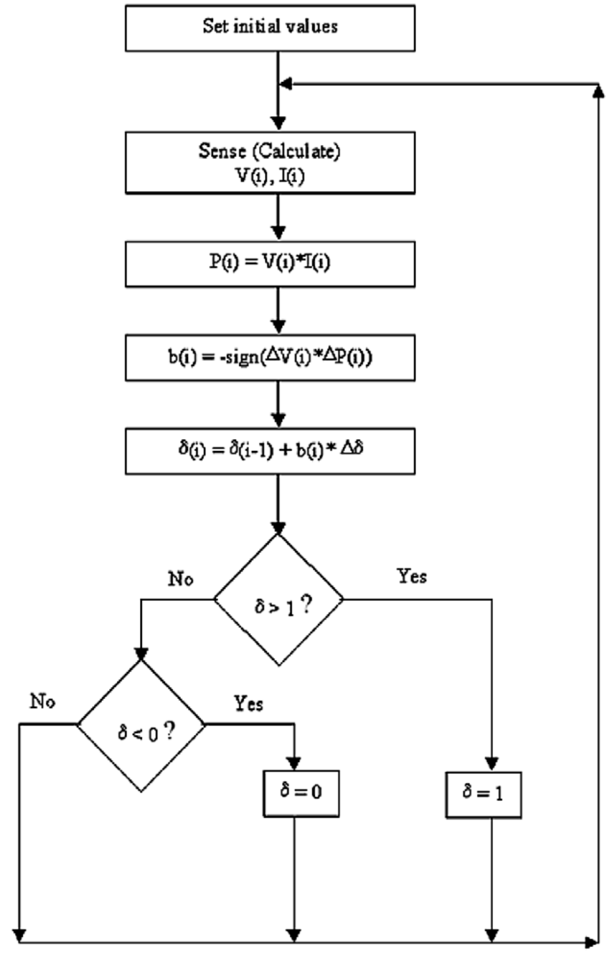

Fig. 5. Flow chart of the MPPT P&O-oriented algorithm.

3.2. The developed system

The whole developed system is shown in Fig. 11. To explain its operation, the system will be analyzed by blocks. Fig. 6 shows the circuit that, from the voltage and current measures at the PV array output, generates a reference signal, V_{ref}, which will then be used in another block to generate a PWM signal.

From the voltage and current measures at the array output (V, I), the variable power, P, is generated by using the multiplier "Mult. 1". Two differentiators followed by two comparators generate the value of the functions $sign(dV)$ and $sign(dP)$. These two signals are multiplied and compared again to generate the analog equivalent of the bit

Table 1
Possible cases and control law to enable the photovoltaic system follow the MPP.

Case	System evolution			Control law ($V \rightarrow V_{MPP}$)		
	$sign(\Delta V)$	$sign(\Delta P)$	$b_i = -sign((\Delta V) * (\Delta P))$	V	$sign(\Delta V)$	δ
$V_A \rightarrow V_B$	+1	+1	−1	↑	+1	↓
$V_B \rightarrow V_A$	−1	−1	−1	↑	+1	↓
$V_C \rightarrow V_D$	+1	−1	+1	↓	−1	↑
$V_D \rightarrow V_C$	−1	+1	+1	↓	−1	↑

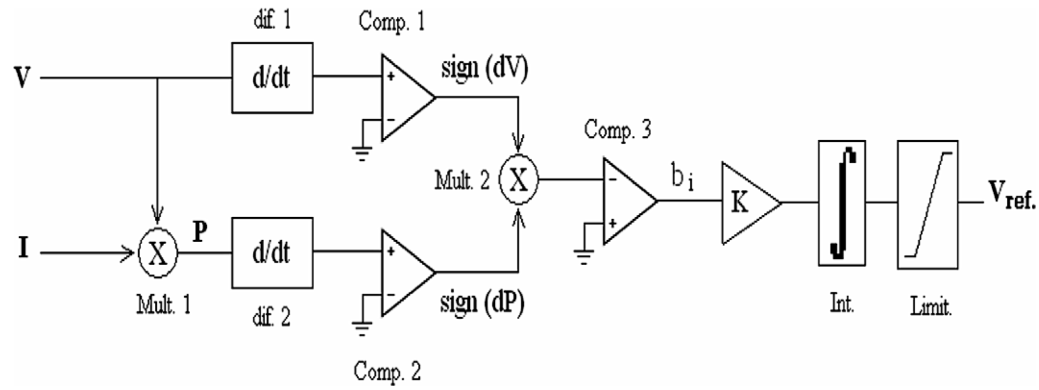

Fig. 6. System generating the reference signal.

"b_i". The iterations of expression (3) are formed by integrating the subsequent b_i. Finally, the output signal is limited in order to maintain it within the appropriate range, generating V_{ref}. This signal can be used as control signal of a PWM generating system (Enrique et al., 2005a,b).

To perform the practical implementation of the developed system, the chip AD633J has been selected as multiplier block. For the comparators, the cheap (approx. 0.5 $) and extensively used op-amp TL082 has been selected. The integrator and differentiator blocks are shown in Fig 7. Both structures are basic in analog electronics. The op-amp TL082 has also been used for their implementation.

A lowpass RC filter has been inserted before each differentiator block to remove part of the harmonic content of the input signals. The output signal, V_{ref}, of the system in Fig. 6 is used as reference voltage for a PWM generator (see Fig. 8), so that its duty cycle can be adjusted.

The output PWM signal of the circuit in Fig. 8 allows controlling the behavior of the DC/DC converter. This converter (boost-type, in this case) is shown in Fig. 9 connected to a 25 Ω load.

To reduce the price of the sensors, the voltage input is taken from the photovoltaic array using a high impedance voltage divider with a voltage follower. The measurement of the current variable is performed by measuring the voltage fall in a very low value resistance, located at one of the PV array terminals. This measure must be amplified before reaching the multiplier. For this purpose, a very low offset voltage precision op-amp OP27 has been used (see Fig. 10).

Fig. 11 shows the diagram of the whole developed MPPT system.

4. Simulations

The developed system has been verified using PSpice®. The photovoltaic generator has been implemented using ABM blocks (*Analog Behavioral Modeling*). The parameters of the generator model correspond to the "BP Saturno" module ($ns = 60$ and $np = 1$) (CIEMAT, 2000). Fig. 12 presents the model and *I–V* and *P–V* curves of the module used at 21 °C and 1000 W/m^2. Table 2 shows the MPP power and current (P_{MPP} and I_{MPP}, respectively) for different levels of radiation and constant temperature.

To verify the correct operation of the system, fast variations in the incident radiation have been applied to it (see Fig. 13). Observe that during start-up, an initial rise of 688.7 W/m^2 in the incident radiation ($P_{MPP} = 55.2$ W) is reached by the system in approximately 10 ms. Once the maximum power point has been reached, the system maintains it even for variations higher than 5×10^3 W/m^2/s, much higher than those present in nature. Additionally, it can be observed that the system presents a high precision, since the actual trajectory of the MPP and the one intended do not have practically noticeable differences. Fig. 14 shows the current obtained with the tracker system.

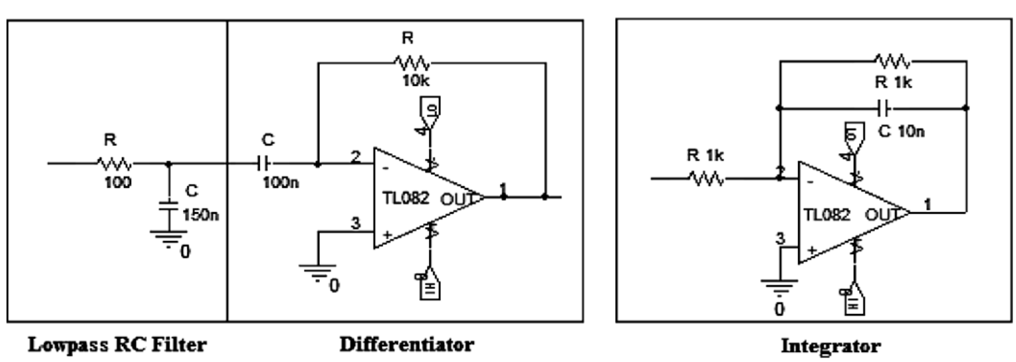

Fig. 7. Differentiator and integrator blocks used.

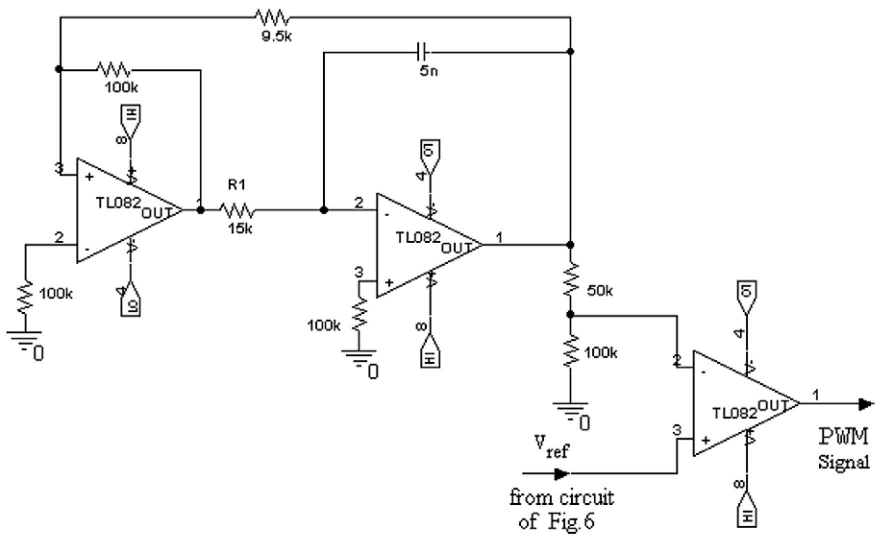

Fig. 8. System generating the PWM signal.

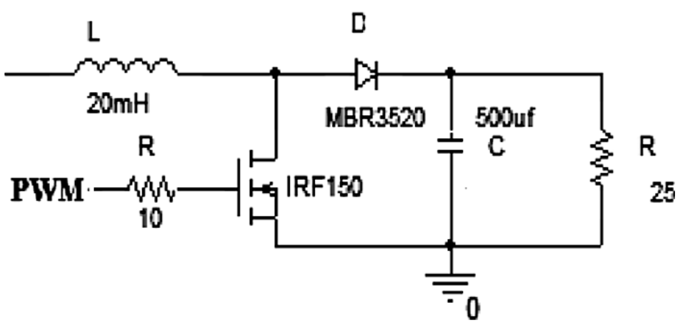

Fig. 9. Boost converter used.

With this sudden start-up, the tracking system is able to obtain efficiencies superior to 97.2% in the first 100 ms. Once the MPP has been reached (during the first milliseconds of the start-up) the system presents a tracking efficiency η higher than 99% (99.99%), even for variations in the incident radiation as fast and extreme as those shown in Fig. 13. This efficiency is superior to 81–85% of a classical "P&O" system (*Perturb and Observed*), superior to 88–89% of an "InC" system (*Incremental Conductance*) and to 73–85% of a "CV" system (*Constant Voltage*) (Hohm and Ropp, 2002). In Fig. 15, note how the system is able to adjust automatically the duty cycle of the PWM signal.

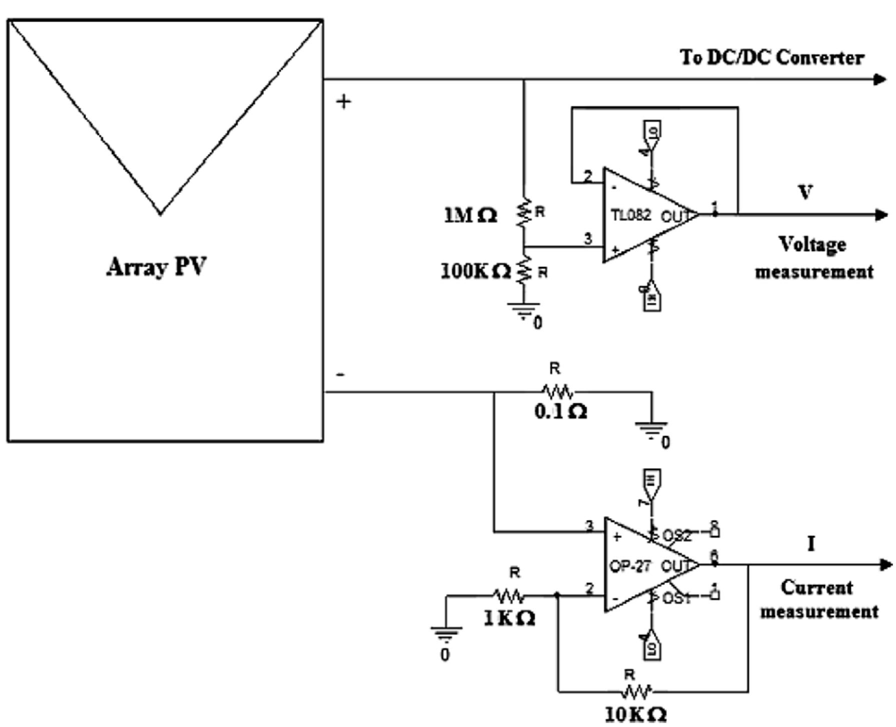

Fig. 10. Measure of variables V and I.

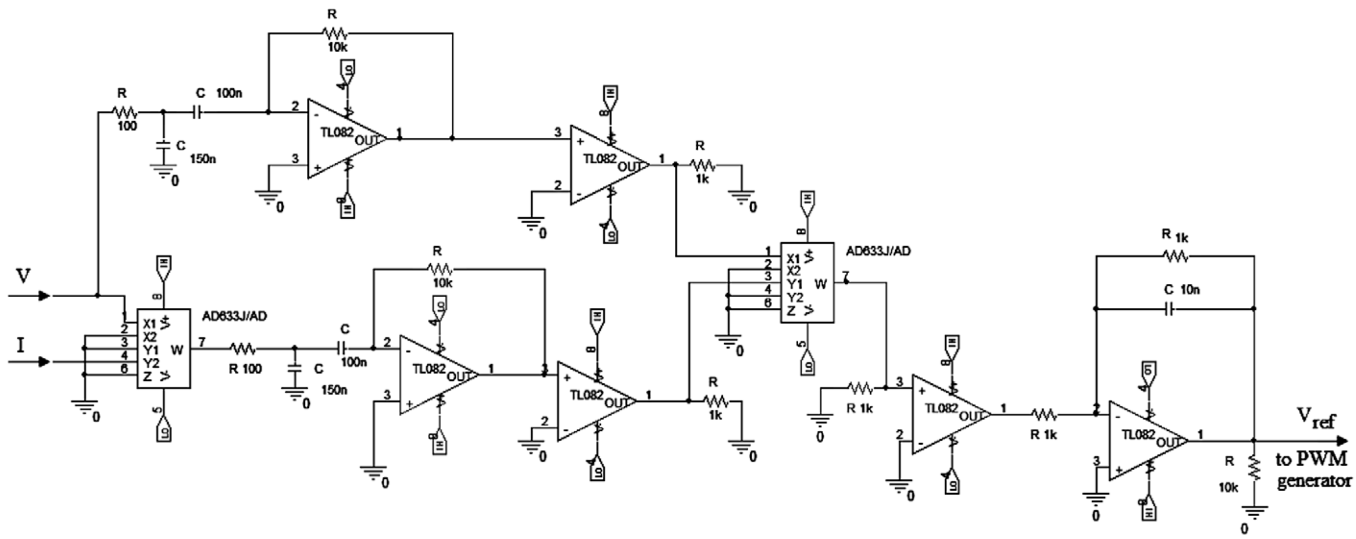

Fig. 11. Diagram of the whole developed system.

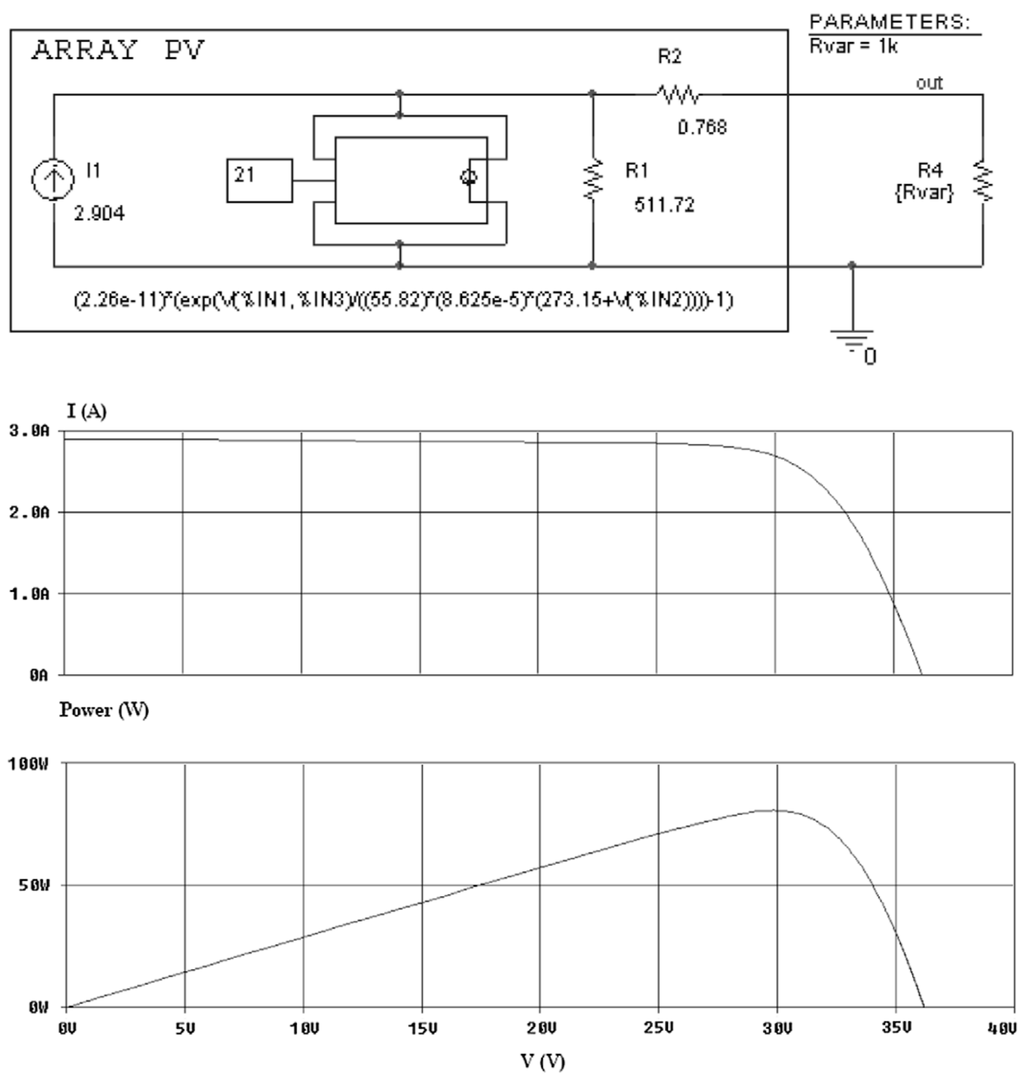

Fig. 12. Model and I–V and P–V curves of the "BP Saturno" module.

Table 2
P_{MPP} and I_{MPP} for different levels of radiation and constant temperature corresponding to the "BP Saturno" generator.

Temperature (°C)	Radiation (W/m^2)	P_{MPP} (W)	I_{MPP} (A)
21	688.7	55.2	1.86
21	1000	80.6	2.71
21	1721.8	136.2	4.76

5. Conclusions

In this work, the design of a new maximum power point (MPP) tracking system for photovoltaic systems has been developed. The system is an analog version of the tracking "P&O-oriented" algorithm. From the results obtained by simulation, it can be concluded that the developed system presents an excellent precision and speed in the MPP track-

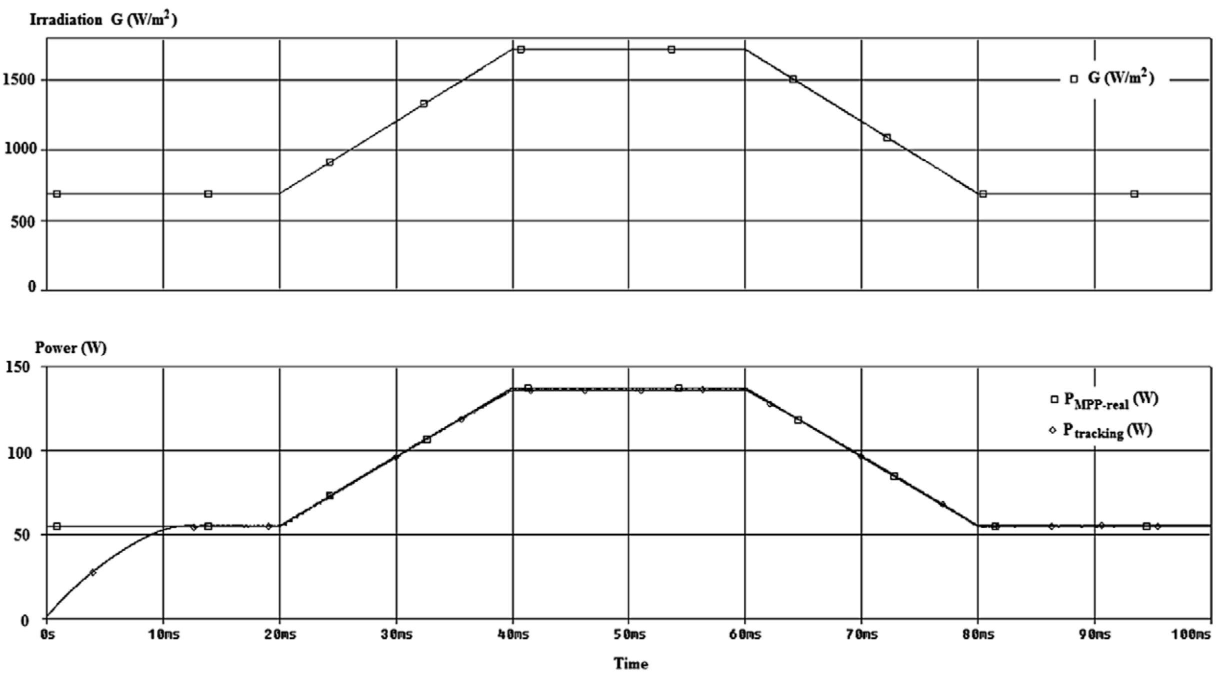

Fig. 13. Top chart: applied variations in the incident radiation. Bottom chart: comparative between the actual trajectory of the MPP and that followed by the developed system for variations in the incident radiation.

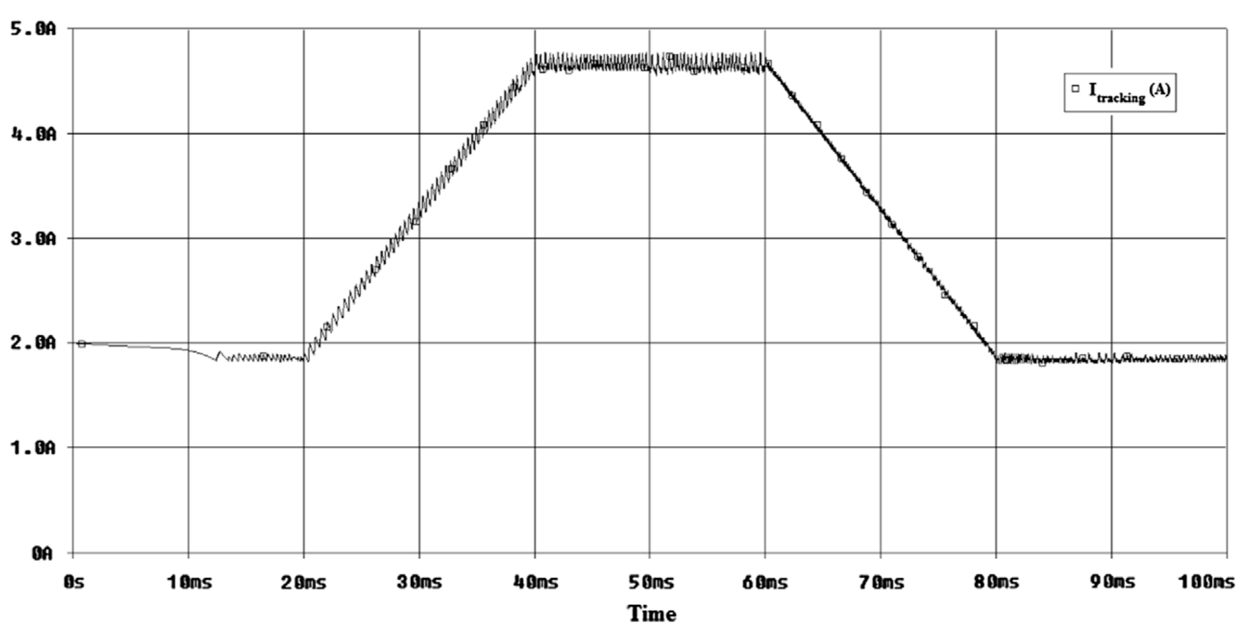

Fig. 14. Current supplied by the system for variations in the incident radiation.

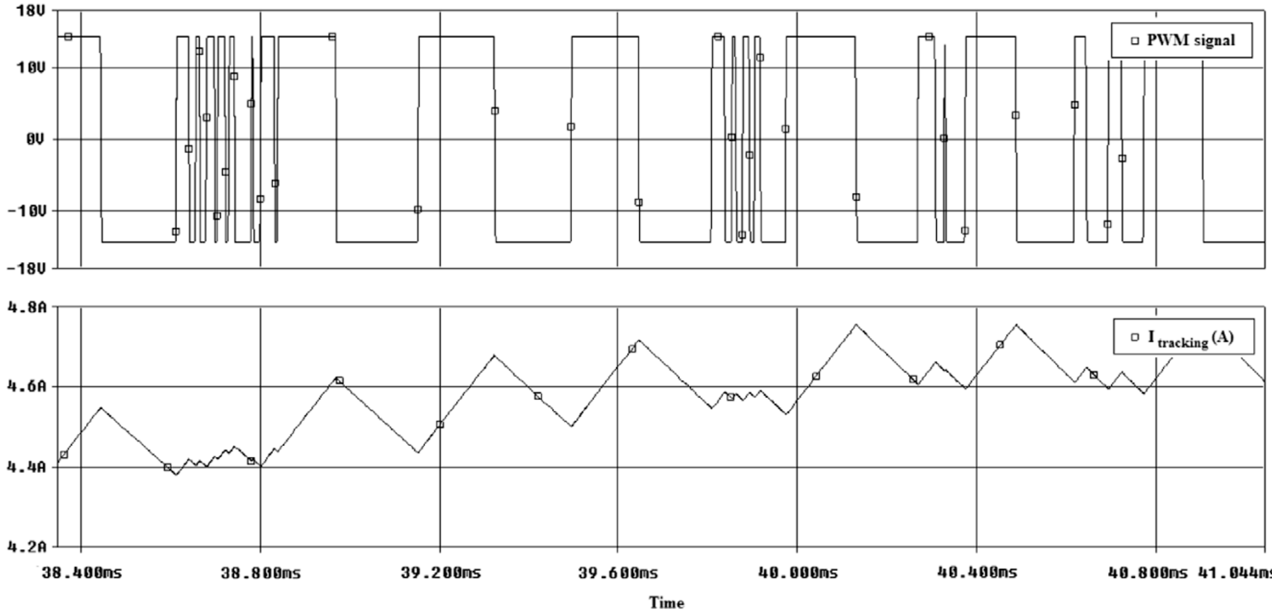

Fig. 15. Top chart: PWM signal generated by the developed system during a certain interval. Bottom chart: current supplied by the system during the time interval.

ing, even for very sudden variations in the levels of incident radiation, so increasing the total energy performance of the installation. The system is able to reach the MPP in the first 10 ms, getting high efficiency values practically from the start-up. Once the system has reached the MPP, the efficiency is superior to 99%, improving the ones obtained by other methods ("P&O", "InC", "CV"). This quality, along with its high simplicity and low price, makes the proposed system highly suitable for use in any kind of photovoltaic installation.

Acknowledgment

The present work is a contribution of the DPI2007 62336/project, funded by The Spanish Ministry of Education.

References

Abou El Ela, M., Roger, J., 1984. Optimization of the function of a photovoltaic array using a feedback control system. Solar Cells: Their Science, Technology, Applications and Economics 13 (2), 185–195.

Alonso, G.M.C., 1998. El Generador Fotovoltaico. CIEMAT, Serie de Ponencias, Editorial CIEMAT, Madrid.

Andersen, M., Alvsten, B., 1995. 200 W low cost module integrated utility interface for modular photovoltaic energy systems. In: IECON: Proceedings of the 1995 IEEE 21st International Conference on Industrial Electronics, Control and Instrumentation, vol. 1, no. 1, pp. 572–577.

Andujar, J.M., Enrique, J.M., Bohórquez, M.A.M., Durán, E., 2005. Sistema de Control de Bajo Costo para el Seguimiento del punto de Máxima Potencia en Sistemas Fotovoltaicos. In: Proc. De las XXVI Jornadas de Automática, Alicante, España. ISBN: 84-689-0730-8.

Brambilla, A., et al., 1998. New approach to photovoltaic arrays maximum power point tracking. In: Proceedings of the 30th IEEE Power Electronics Conference, pp. 632–637.

CIEMAT: Fundamentos, dimensionado y aplicaciones de la energía solar fotovoltaica, Cap. 11, Editorial CIEMAT, Madrid 2000.

Durán, E., Galán, J., Andújar, J.M., Sidrach-de-Cardona, M., 2008. A new method to obtain *I–V* characteristics curves of photovoltaic modules based on SEPIC and Cuk converters. EPE Journal 18 (2), 5–15.

Durán, E, Andújar, J.M., Galán, J., Sidrach-de-Cardona, M., 2009. Methodology and experimental system for measuring and displaying *I–V* characteristic curves of PV facilities. Progress in Photovoltaics. Available from: <http://dx.doi.org/10.1002/pip.909/>.

Enrique, J.M., Durán, E., Sidrach, M., Andújar, J.M., 2005a. A new approach to obtain *I–V* and *P–V* curves of PV panels by using DC–DC converters. In: 31st IEEE Photovoltaic Specialists Conference, January 3–7, 2005.

Enrique, J.M., Sidrach-de-Cardona M., Durán E., Bohórquez M.A, Carretero, J.E., Andújar J.M., 2005. An optimum configuration of DC/DC converters to use in photovoltaics facilities. In: 20th European Photovoltaic Solar Energy Conference and Exhibition, EUPVSEC 2005, Barcelona, Junio 2005.

Enrique, J.M., Durán, E., Sidrach-de-Cardona, M., Andujar, J.M., 2007. Theoretical assessment of the maximum power point tracking efficiency of photovoltaic facilities with different converter topologies. Solar Energy 81 (1), 31–38.

Enslin, J.H.R., Wolf, M., Swiegers, W., 1997. Integrated photovoltaic maximum power point tracking converter. IEEE Transactions on Industrial Electronics 44 (6), 769–773.

Hohm, D.P., Ropp, M.E., 2002. Comparative study of maximum power point tracking algorithms. Progress in Photovoltaics: Research and Applications.

Kawamura, T., et al., 1997. Analysis of MPPT characteristics in photovoltaic power systems. Solar energy materials and solar cells. In: Proceedings of the 1996 9th International Photovoltaic Science and Engineering Conference, PVSEC-9 1997, vol. 47, no. 14, pp. 155–165.

Kim, Y., Jo, H., Kim, D., 1996. A new peak power tracker for cost-effective photovoltaic power systems. IEEE Proceedings 3 (1), 1673–1678.

Koizumi, H., Mizuno, T., Kaito, T., Noda, Y., Goshima, N., Kawasaki, M., Nagasaka, K., Kurokawa, K., 2006. A novel microcontroller for grid-connected photovoltaic systems. IEEE Transactions on Industrial Electronics 53 (6), 1889–1897. doi:10.1109/TIE.2006.885526.

Martínez, M.A., Andújar, J.M., 2009. A new and inexpensive temperature measuring system. Application to photovoltaic solar facilities. Solar Energy 83 (6), 883–890.

Martínez, M.A., Andújar, J.M., Enrique, J.M., 2009. A new and inexpensive pyranometer for the visible spectral range. Sensors-Basel 9 (6), 4615–4634.

Mutoh, N., Inoue, T., 2007. A control method to charge series-connected ultraelectric double-layer capacitors suitable for photovoltaic generation systems combining MPPT control method. IEEE Transactions on Industrial Electronics 54 (1), 374–383. doi:10.1109/TIE.2006.885149.

Mutoh, N., Ohno, M., Inoue, T., 2006. A method for MPPT control while searching for parameters corresponding to weather conditions for PV generation systems. IEEE Transactions on Industrial Electronics 53 (4), 1055–1065. doi:10.1109/TIE.2006.878328.

Noguchi, T., Togashi, S., Nakamoto, R., 2002. Short-current pulse-based maximum-power-point tracking method for multiple photovoltaic-and-converter module system. IEEE Transactions on Industrial Electronics 49 (1), 217–223. doi:10.1109/41.982265.

van der Merwe, L., van der Merwe, G., 1998. Maximum power point tracking – implementation strategies. In: Proceedings of the IEEE International Symposium on Industrial Electronics, vol. 1, no. 1, 214–217.

Xiao, W., Lind, M.G.J., Dunford, W.G., Capel, A., 2006. Real-time identification of optimal operating points in photovoltaic power systems. IEEE Transactions on Industrial Electronics 53 (4), 1017–1026. doi:10.1109/TIE.2006.878355.

Xiao, Weidong, Ozog, N., Dunford, W.G., 2007. Topology study of photovoltaic interface for maximum power point tracking. IEEE Transactions on Industrial Electronics 54 (3), 1696–1704. doi:10.1109/TIE.2007.894732.

Xiao, W., Dunford, W.G., Palmer, P.R., Capel, A., 2007. Application of centered differentiation and steepest descent to maximum power point tracking. IEEE Transactions on Industrial Electronics 54 (5), 2539–2549. doi:10.1109/TIE.2007.899922.